

# Structural chemistry of the cation-ordered perovskites $\text{Sr}_2\text{CaMo}_{1-x}\text{Te}_x\text{O}_6$ ( $0 \leq x \leq 1$ )

Timothy J. Prior, Victoria J. Couper, Peter D. Battle\*

*Inorganic Chemistry Laboratory, University of Oxford, South Parks Road, Oxford, Oxfordshire OX1 3QR, UK*

Received 1 October 2004; received in revised form 29 October 2004; accepted 31 October 2004

## Abstract

The crystal structures of  $\text{Sr}_2\text{CaMoO}_6$  and  $\text{Sr}_2\text{CaTeO}_6$  have been determined at room temperature by neutron powder diffraction. Both compounds crystallize in the perovskite structure with a rock-salt ordered array of  $\text{Ca}^{2+}$  and  $M^{6+}$  cations ( $M = \text{Mo}, \text{Te}$ ) on the six-coordinate sites (space group  $P2_1/n$  (no. 14); for  $M = \text{Mo}$ ,  $a = 5.76228(7)$ ,  $b = 5.84790(7)$ ,  $c = 8.18707(9)$  Å,  $\beta = 90.194(1)^\circ$ , for  $M = \text{Te}$ ,  $a = 5.79919(9)$ ,  $b = 5.83756(8)$ ,  $c = 8.2175(1)$  Å,  $\beta = 90.194(1)^\circ$ ). Compositions in the solid solution  $\text{Sr}_2\text{CaMo}_{1-x}\text{Te}_x\text{O}_6$  have been synthesized and shown by X-ray diffraction to adopt the same ordered structure. The results are used in a discussion of the cation oxidation states in  $\text{Ca}_2\text{FeMoO}_6$  and to establish the similarity between the structural chemistry of hexavalent Mo and Te. © 2004 Elsevier Inc. All rights reserved.

**Keywords:** Cation-ordered perovskite; Neutron diffraction; Molybdate; Tellurate; Elpasolite

## 1. Introduction

The perovskite structure is central to solid-state oxide chemistry. It is able to accommodate a wide variety of elements and the composition can often be manipulated in order to optimize some chosen property, for example conductivity, magnetism, dielectric behavior, or catalytic activity. These manipulations often result in compositions which can be written as  $\text{A}_2\text{BB}'\text{O}_6$ , where the six-coordinate sites are occupied by a 1:1 ratio of two cations,  $B$  and  $B'$ , and the larger (ideally) 12-coordinate sites are occupied by a cation,  $A$  [1]. The properties of this compound will depend on the electron configuration of  $B$  and  $B'$ , but also on whether they are distributed randomly or in an ordered manner over the octahedral sites. However, these two criteria are not independent, with the available evidence suggesting that a cation with an open  $d$ -shell, for example  $\text{Fe}^{3+}$ , is more likely to form an ordered array with a  $d^{10}$  cation, for example  $\text{Sb}^{5+}$ , than with a  $d^0$  cation, for example  $\text{Ta}^{5+}$  [2]; the  $d^0$  cation

does however order with  $d^{10} \text{Ga}^{3+}$  [3]. The tendency of  $d^{10}$  cations to form an ordered array is further demonstrated by the fact that both  $\text{Fe}^{3+}$  and  $\text{Cu}^{2+}$  order to a greater extent with  $\text{Sb}^{5+}$  than with  $\text{Ru}^{5+}$  [4–6], even though it has been shown that the latter two cations are similar in size and that they can show very similar structural chemistry in the perovskite structure [7,8]. The degree of cation ordering depends on the size and charge difference between the species involved, and the examples cited above all involve differences in formal charge of 2 or 3 units. Examples involving a charge difference of four units are relatively rare, but the cation pairs  $\text{Ca}^{2+}/\text{Mo}^{6+}$  and  $\text{Ca}^{2+}/\text{Te}^{6+}$  can be used to compare the behavior of  $d^0$  and  $d^{10}$  cations in such circumstances.  $\text{Sr}_2\text{CaTeO}_6$  and  $\text{Sr}_2\text{CaMoO}_6$  have both been described previously [9,10] as ordered perovskites. The former was listed as having a cubic structure, with no detail given, whereas on the basis of X-ray powder diffraction data, the latter was assigned to the orthorhombic space group  $Pmm2$ . We have reinvestigated these phases by neutron powder diffraction and we show below that they are isostructural, monoclinic, cation-ordered perovskites. Furthermore, in order to

\*Corresponding author. Fax: +44 1865 272690.

E-mail address: [peter.battle@chem.ox.ac.uk](mailto:peter.battle@chem.ox.ac.uk) (P.D. Battle).

emphasize the similarities in the structural chemistries of *d*- and *p*-block elements from the second long period, we have prepared and characterized the solid solution  $\text{Sr}_2\text{CaMo}_{1-x}\text{Te}_x\text{O}_6$ .

## 2. Experimental

### 2.1. Synthesis

Polycrystalline samples used in this study were prepared by conventional solid-state synthesis techniques, using stoichiometric quantities of the appropriate oxides or carbonates: strontium oxide (99.994%), calcium carbonate (99.999%), molybdenum trioxide (99.9995%), and tellurium dioxide (99.9995%). Reactant mixtures were intimately ground using an agate pestle and mortar and heated in air at 700 °C overnight to decompose the carbonates. Samples were ground again and pressed into pellets and fired in air for 24 h at each of the following firing temperatures with intermittent regrinding: 900, 1000, 1050, 1100, 1150, and 1200 °C.

### 2.2. Characterization

The progress of each synthesis was charted by X-ray powder diffraction using a Philips diffractometer operating with Cu  $K\alpha$  radiation. Relatively high resolution data to be used in quantitative analyses were collected using a Siemens D5000 diffractometer nominally operating with Cu  $K\alpha_1$  radiation over the angular range  $10 \leq 2\theta / ^\circ \leq 125$  with a step size of  $\Delta 2\theta = 0.02^\circ$ . However, imperfect monochromation introduced a contribution of approximately 2%  $K\alpha_2$  which was allowed for in the data analysis.

Neutron powder diffraction data were collected from  $\text{Sr}_2\text{CaMoO}_6$  and  $\text{Sr}_2\text{CaTeO}_6$  at 300 K on ca. 4.6 g samples using the instrument D2b at the Institut Laue Langevin, Grenoble, France. D2b is a medium flux, high-resolution diffractometer which operates at a wavelength of 1.595 Å. Useful data were collected over an angular range  $15 \leq 2\theta / ^\circ \leq 150$ , with a stepsize  $\Delta 2\theta = 0.05^\circ$ . Samples were loaded inside vanadium cans for data collection. Rietveld refinement [11] of the crystal structures was carried out using the GSAS [12] suite of programs. Backgrounds were fitted using a shifted Chebyshev polynomial of the first kind. Peak shapes were modelled using a pseudo-Voigt function. Atomic positions, isotropic displacement parameters and the appropriate profile parameters were refined.

## 3. Results

The compounds  $\text{Sr}_2\text{CaMoO}_6$  and  $\text{Sr}_2\text{CaTeO}_6$  were successfully synthesized in air by standard ceramic

techniques, but careful analysis of relatively high resolution X-ray diffraction data suggested the previous assignments of the symmetries of these phases were both incorrect. The previously reported [9,13] orthorhombic model in *Pmm2* was initially employed to fit the X-ray data for  $\text{Sr}_2\text{CaMoO}_6$ . However, this provided a rather poor fit to the data, and close inspection suggested a reduction in the symmetry of the model was necessary. A LeBail extraction in space group *P222* converged with  $\chi^2 = 11.42$ , while a refinement in the monoclinic space group *P2* ( $\beta \approx 90^\circ$ ) converged with  $\chi^2 = 1.750$ . A model in *P2<sub>1</sub>/n*, which is common for ordered double perovskites (elpasolite structure) [1], was therefore employed and this yielded a greatly improved fit to the observed data. Rietveld analysis of neutron diffraction data confirmed the choice of space group; the final refinement converged with  $\chi^2 = 3.764$  and  $R_{\text{wp}} = 0.0335$ . The fit to the neutron diffraction data is given in Fig. 1a. The elpasolite unit cell is related to that of a simple cubic perovskite in the following way:  $a \sim a_0\sqrt{2}$ ,  $b \sim a_0\sqrt{2}$ ,  $c \sim 2a_0$ ,  $\beta \sim 90^\circ$ , where  $a_0$  is the perovskite cell parameter. In terms of the formalism devised by Glazer [14] and extended by Woodward [15]

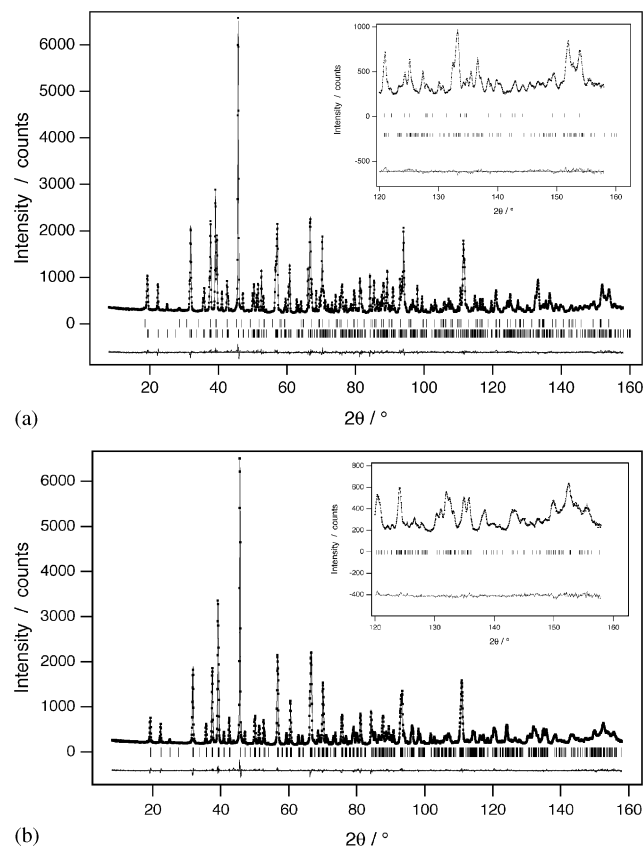


Fig. 1. Observed (·), calculated (—) and difference neutron powder diffraction profiles for (a)  $\text{Sr}_2\text{CaMoO}_6$  and (b)  $\text{Sr}_2\text{CaTeO}_6$  at room temperature. Tick marks indicate positions of allowed reflections; in (a) the upper set correspond to the  $\text{SrMoO}_4$  impurity, the lower set to the main phase.

this symmetry results in a negative octahedral tilt sequence along two of the pseudo-cubic axes and a positive tilt sequence along the third. Double perovskites adopt the distorted elpasolite structure where there is rock salt ordering (Fig. 2) of the *B*-site cations, in particular where there are large differ-

ences in size and charge on these cations. In the present case the ions  $\text{Ca}^{2+}$  and  $\text{Mo}^{6+}$  are ordered on the *B* site and  $\text{Sr}^{2+}$  cations occupy the *A* sites exclusively. Crystal data and atomic positions are given in Table 1. Selected bond lengths and angles are given in Table 2. Approximately 1.8(2) % by weight of  $\text{SrMoO}_4$  was present in the sample and this was allowed for in the data analysis.

An assignment of cubic symmetry for  $\text{Sr}_2\text{CaTeO}_6$  was made in an early report [10] of its structure, but it is clear from our X-ray diffraction data that this is incorrect. By analogy with  $\text{Sr}_2\text{CaMoO}_6$  a monoclinic elpasolite model was initially utilized and this provided a good fit to the observed data. Rietveld refinement against X-ray data showed  $\beta = 90.194(1)^\circ$  (precluding an orthonormal crystal system) and confirmed the choice of model. Neutron diffraction data were analyzed using the Rietveld method and an excellent fit was obtained:  $\chi^2 = 3.404$  and  $R_{\text{wp}} = 0.0345$ . Structural parameters are detailed in Table 1, bond lengths and angles in Table 2, and the fit is shown in Fig. 1b. The structure of the tellurium compound is analogous to the molybdenum-containing phase and contains  $\text{Sr}^{2+}$  cations on the *A*-sites with a rock-salt ordered array of  $\text{Ca}^{2+}$  and  $\text{Te}^{6+}$  on the *B*-sites.

It proved possible to obtain the solid solution  $\text{Sr}_2\text{CaMo}_{1-x}\text{Te}_x\text{O}_6$  by the same synthetic method. Rietveld analysis of X-ray diffraction data for the compositions  $x = 0.1, 0.2,$  and  $0.5$  suggested these compounds all crystallize with an ordered perovskite structure. There is a steady change in the colour of samples from bright yellow ( $x = 0$ ) to very pale yellow ( $x = 1$ ) across the series. There is no evidence for ordering of the molybdenum and tellurium on the *B'* site from the diffraction data. Unit cell parameters derived from X-ray data are given in Table 3.

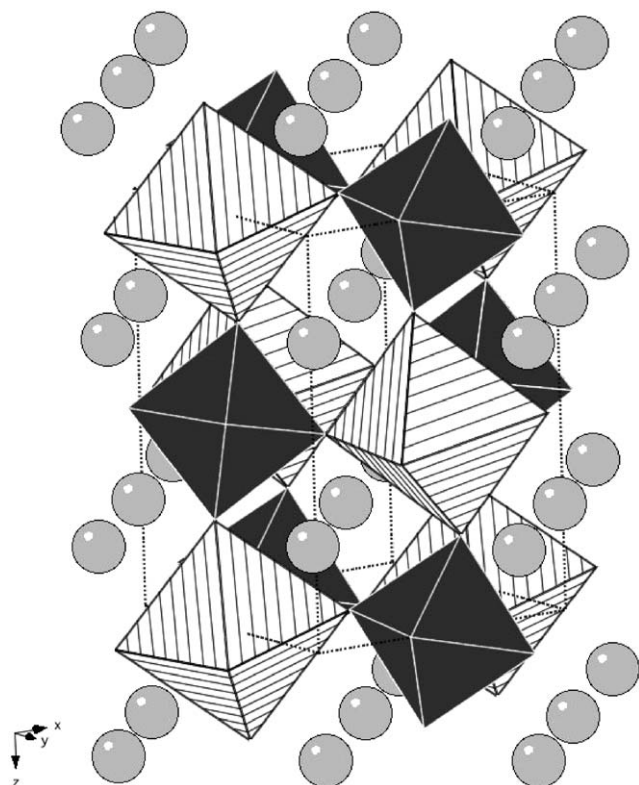


Fig. 2. Crystal structure of  $\text{Sr}_2\text{CaMO}_6$  ( $M = \text{Mo}$  or  $\text{Te}$ ). Sr atoms are shown as gray spheres.  $\text{CaO}_6$  octahedra are hatched and  $\text{MO}_6$  octahedra are black.

Table 1  
Structural parameters for  $\text{Sr}_2\text{CaMO}_6$  ( $M = \text{Mo}, \text{Te}$ ) derived from neutron powder diffraction data

Compound	$\text{Sr}_2\text{CaMoO}_6$					$\text{Sr}_2\text{CaTeO}_6$				
Space group	$P2_1/n$ (no. 14)					$P2_1/n$ (no. 14)				
$a/\text{\AA}$	5.76228(7)					5.79919(9)				
$b/\text{\AA}$	5.84790(7)					5.83756(8)				
$c/\text{\AA}$	8.18707(9)					8.2175(1)				
$\beta/^\circ$	90.194(1)					90.194(1)				
Cell volume/ $\text{\AA}^3$	275.880(8)					278.19(1)				
$R_{\text{wp}}$	0.0335					0.0345				
Atom	Wyckoff position	$x$	$y$	$z$	Uiso/ ( $\text{\AA}^2$ )	$x$	$y$	$z$	Uiso/ ( $\text{\AA}^2$ )	
Sr	$4e$	0.5080(2)	0.5383(1)	0.2500(2)	0.0123(2)	0.5070(3)	0.5316(1)	0.2486(2)	0.0102(2)	
Ca	$2c$	0	$\frac{1}{2}$	0	0.0096(5)	0	$\frac{1}{2}$	0	0.0083(5)	
$M$ (Mo/Te)	$2d$	$\frac{1}{2}$	0	0	0.0055(3)	$\frac{1}{2}$	0	0	0.0051(4)	
O1	$4e$	0.2328(2)	0.1887(2)	0.9618(2)	0.0131(3)	0.2362(2)	0.1941(2)	0.9636(2)	0.0120(4)	
O2	$4e$	0.3157(2)	0.7307(2)	0.9558(2)	0.0122(3)	0.3109(3)	0.7334(3)	0.9590(2)	0.0123(3)	
O3	$4e$	0.4232(2)	0.9764(2)	0.2269(2)	0.0118(3)	0.4286(2)	0.9805(2)	0.2277(2)	0.0105(3)	

For  $\text{Sr}_2\text{CaMoO}_6$ , 1.8(2) % by weight of  $\text{SrMoO}_4$  was present which was allowed for in the data analysis.

Table 2  
Selected bond lengths (Å) and bond angles (°) for Sr<sub>2</sub>CaMoO<sub>6</sub> (*M* = Mo, Te)

	Sr <sub>2</sub> CaMoO <sub>6</sub>	Sr <sub>2</sub> CaTeO <sub>6</sub>	Sr–O distances	Sr <sub>2</sub> CaMoO <sub>6</sub>	Sr <sub>2</sub> CaTeO <sub>6</sub>
<i>M</i> –O1 × 2	1.9187(13)	1.9266(13)	Sr–O1	2.879(2)	2.917(2)
<i>M</i> –O2 × 2	1.9330(12)	1.9328(14)		2.794(2)	2.800(2)
<i>M</i> –O3 × 2	1.9157(13)	1.9214(15)		2.536(2)	2.571(2)
Mean <i>M</i> –O	1.9225(7)	1.9269(8)		3.498(2)	3.436(2)
∠ O1– <i>M</i> –O2	89.88(6), 90.12(6)	89.80(7), 90.20(7)	Sr–O2	2.878(2)	2.886(2)
∠ O1– <i>M</i> –O3	89.33(6), 90.67(6)	89.29(8), 90.71(8)		2.5211(19)	2.536(2)
∠ O2– <i>M</i> –O3	89.69(6), 90.32(6)	89.90(6), 90.10(6)		2.790(2)	2.820(2)
Ca–O1 × 2	2.2838(12)	2.2707(13)		3.542(2)	3.498(2)
Ca–O2 × 2	2.2945(12)	2.2857(14)	Sr–O3	3.3273(13)	3.254(14)
Ca–O3 × 2	2.2823(13)	2.2769(14)		2.6150(14)	2.6652(14)
Mean Ca–O	2.2869(7)	2.2778(8)		2.5188(16)	2.5519(18)
				3.3021(16)	3.2916(18)

Table 3  
Refinement statistics and crystal data for Sr<sub>2</sub>CaMo<sub>1–*x*</sub>Te<sub>*x*</sub>O<sub>6</sub> from X-ray powder diffraction data

<i>x</i>	χ <sup>2</sup>	R <sub>wp</sub> (%)	<i>a</i> (Å)	<i>b</i> (Å)	<i>c</i> (Å)	β (°)	Cell volume (Å <sup>3</sup> )
0	1.750	14.48	5.76108(5)	5.84488(5)	8.18429(7)	90.198(1)	275.586(4)
0.1	2.083	15.51	5.7624(1)	5.8403(1)	8.1845(2)	90.203(3)	275.44(1)
0.2	2.495	17.79	5.7652(1)	5.8379(1)	8.1875(2)	90.209(2)	275.565(9)
0.5	1.977	14.93	5.7854(2)	5.8353(2)	8.2101(2)	90.217(3)	277.19(1)
1	1.528	13.17	5.7959(1)	5.8335(1)	8.2131(1)	90.194(1)	277.69(1)

#### 4. Discussion

This is the first full analysis of the crystal structures of Sr<sub>2</sub>CaTeO<sub>6</sub> and Sr<sub>2</sub>CaMoO<sub>6</sub>. The only previous report of the former [10] merely presents the unit cell parameter of a cubic crystal structure. The most recent study of the latter reports an orthorhombic structure based on the peak positions in an X-ray powder diffraction pattern [9]. No quantitative analysis of the intensity data was presented, although the result was used, with others, to construct a “fitness factor” to discriminate the crystal symmetry of double perovskites—in effect an alternative to the tolerance factor. We are confident that these previous reports overestimate the symmetry of both compounds and that our conclusion that they are both monoclinic with 1:1 *B*-site ordering is correct. The overestimation of the symmetry in the previous study demonstrates the importance of quantitative intensity analysis, emphasizes the value of high-resolution neutron powder diffraction in oxide chemistry, and casts serious doubt on the validity of the fitness-factor concept, a concept which we have shown to be based on incorrect structural information.

Tellurium is known to occur in ordered perovskites, some of which are structurally complex, for example Pb<sub>2</sub>MgTeO<sub>6</sub> [16]. Only one composition, Na<sub>2</sub>SnTeO<sub>6</sub>,

has previously been described in space group *P*2<sub>1</sub>/*n* and in that case the use of X-ray data necessitated the imposition of a strict constraint on the Te–O bond length [17]. The mean value determined in the present work is comparable to those found in other compounds containing TeO<sub>6</sub> octahedra, for example Ca<sub>3</sub>TeO<sub>6</sub> [18], *d* = 1.919(6) Å; CaTeO<sub>4</sub> [19] *d* = 1.94(8) Å; SrTeO<sub>4</sub> [19] *d* = 1.95(6) Å. Similarly, Mo-containing ordered perovskites are known, although not many have been fully characterized. Ca<sub>2</sub>FeMoO<sub>6</sub> is the only composition reported to crystallize in *P*2<sub>1</sub>/*n* [20]. This material is of contemporary interest, having shown a magnetoresistance of 30% at room temperature in a magnetic field of 9 T. There is some debate as to whether it should be described at Fe<sup>3+</sup>/Mo<sup>5+</sup> or Fe<sup>2+</sup>/Mo<sup>6+</sup>. The Mo–O bond lengths in Sr<sub>2</sub>CaMoO<sub>6</sub>, unambiguously containing Mo<sup>6+</sup> with a bond valence (BV) [21] sum of 5.83, are significantly shorter than those in Ca<sub>2</sub>FeMoO<sub>6</sub>, at room temperature, even though the latter has a smaller unit cell volume. This supports the assertion that Ca<sub>2</sub>FeMoO<sub>6</sub> contains Mo<sup>5+</sup>.

Ca<sup>2+</sup> is more often found on the *A* site of the perovskite structure, but it has been observed occupying the *B* site in other compounds, for example Ca<sub>2</sub>LaRuO<sub>6</sub> [22] which is better written as (CaLa)[CaRu]O<sub>6</sub>. The mean Ca–O bond length in that compound (2.274 Å) is

in reasonable agreement with those listed in Table 2. BV calculations suggests that the  $\text{Ca}^{2+}$  ions in both  $\text{Sr}_2\text{CaMoO}_6$  and  $\text{Sr}_2\text{CaTeO}_6$  are “overbonded” with BV sums of 2.23 and 2.27, respectively. The combined effect of the size and charge difference between  $\text{Ca}^{2+}$  and  $M^{6+}$  ( $M = \text{Te}$  or  $\text{Mo}$ ) is great enough to induce *B*-site ordering in both compounds  $\text{Sr}_2\text{CaMO}_6$  irrespective of whether *M* has a  $d^0$  or  $d^{10}$  electron configuration. This demonstration of the isostructural nature of  $\text{Sr}_2\text{CaMoO}_6$  and  $\text{Sr}_2\text{CaTeO}_6$  together with the existence of the solid solution  $\text{Sr}_2\text{CaMo}_{1-x}\text{Te}_x\text{O}_6$  shows that the similarity demonstrated between pentavalent Ru and Sb can also be recognized in the chemistry of hexavalent Mo and Te. The Mo–O and Te–O bond lengths listed in Table 2 are very similar and suggest that it may be possible to modify the properties of mixed-metal oxides of molybdenum by doping with diamagnetic tellurium. We shall return to this theme in a future publication.

## 5. Supporting information

Further details of the crystal structure investigations can be obtained from the Fachinformationszentrum Karlsruhe, 76344 Eggenstein-Leopoldshafen, Germany, (fax: (49) 7247-808-666; e-mail: [crysdata@fiz.karlsruhe.de](mailto:crysdata@fiz.karlsruhe.de)) on quoting the depository number CSD414435.

## Acknowledgments

We are grateful to EPSRC for financial support under grant GR/R88601 and to E. Suard for experimental assistance at ILL, Grenoble.

## References

- [1] M.T. Anderson, K.B. Greenwood, G.A. Taylor, K.R. Poeppelmeier, *Prog. Solid State Chem.* 22 (1993) 197–233.
- [2] E.J. Cussen, J.F. Vente, P.D. Battle, T.C. Gibb, *J. Mater. Chem.* 7 (1997) 459–463.
- [3] E.J. Cussen, P.D. Battle, *J. Mater. Chem.* 13 (2003) 1210–1214.
- [4] M.P. Attfield, et al., *J. Solid State Chem.* 96 (1992) 344–359.
- [5] M. Gateshki, J.M. Igartua, *Mater. Res. Bull.* 38 (2003) 1893–1900.
- [6] P.D. Battle, T.C. Gibb, C.W. Jones, F. Studer, *J. Solid State Chem.* 78 (1989) 281–293.
- [7] P. Lightfoot, P.D. Battle, *Mater. Res. Bull.* 25 (1990) 89–93.
- [8] S.A. Almaer, P.D. Battle, P. Lightfoot, R.S. Mellen, A.V. Powell, *J. Solid State Chem.* 102 (1993) 375–381.
- [9] Y. Teraoka, M.D. Wei, S. Kagawa, *J. Mater. Chem.* 8 (1998) 2323–2325.
- [10] G. Bayer, *Fortschr. Miner.* 46 (1969) 41–72.
- [11] H.M. Rietveld, *J. Appl. Crystallogr.* 2 (1969) 65–71.
- [12] A.C. Larson, R.B. von-Dreele, *General Structure Analysis System (GSAS)*, Los Alamos National Laboratories, 1990.
- [13] Z.-M. Fu, Z.-W. Li, W.-X. Li, *Wu Li Hsueh Pao* 41 (1992) 938–947.
- [14] A.M. Glazer, *Acta Crystallogr. Sect. B—Struct. Commun.* B 28 (1972) 3384.
- [15] P.M. Woodward, *Acta Crystallogr. Sect. B—Struct. Commun.* 53 (1997) 32–43.
- [16] G. Baldinozzi, P. Sciau, J. Moret, P.A. Buffat, *Solid State Commun.* 89 (1994) 441–445.
- [17] J.H. Park, J.B. Parise, P.M. Woodward, I. Lubomirsky, O. Stafsudd, *J. Mater. Res.* 14 (1999) 3192–3195.
- [18] D. Hottentot, B.O. Loopstra, *Acta Crystallogr. B* 37 (1981) 220–222.
- [19] D. Hottentot, B.O. Loopstra, *Acta Crystallogr. B* 35 (1979) 728–729.
- [20] J.A. Alonso, et al., *Chem. Mater.* 12 (2000) 161–168.
- [21] I.D. Brown, *Acta Crystallogr. Sect. B—Struct. Commun.* 48 (1992) 553–572.
- [22] P.D. Battle, J.B. Goodenough, R. Price, *J. Solid State Chem.* 46 (1983) 234–244.